J Appl Electrochem (2007) 37:1485–1494
DOI 10.1007/s10800-007-9378-1

ORIGINAL PAPER

Activity of selenium modified ruthenium-electrodes and determination of the real surface area

Nicky Bogolowski · Tina Nagel · Barbora Lanova · Siegfried Ernst · Helmut Baltruschat · Kyatanahalli S. Nagabhushana · Helmut Boennemann

Received: 4 November 2006 / Revised: 13 July 2007 / Accepted: 13 July 2007 / Published online: 28 August 2007

Abstract The determination of the surface area of Pt and Ru electrocatalyst surfaces by oxidation of adsorbed CO and by oxidation of a Cu upd layer are compared. The amount of adsorbed CO was determined mass-spectrometrically from the ionic current for CO_2 formation during an oxidative potential sweep. On Ru, the Faradaic charge is too large (by approx. 55%) due to Faradaic effects (oxygen adsorption). For massive Ru electrodes a Cu upd charge of 520 μC cm^{-2} is found after normalization to the area determined by CO oxidation. Using this value, both methods yield identical surface areas for nanoparticulate Ru catalysts. On Ru surfaces (both massive and nanoparticulate) completely covered by Se the amount of Cu upd charge decreases to one fourth of the value observed for pure Ru. Since CO is only adsorbed on free Ru sites and not on Se covered sites, the oxidation charge for the latter can be used to determine the number of free Ru sites, whereas the decrease of the Cu upd charge on Se modified surfaces can be used to calculate the area which is modified by Se. This method, previously tested on the model electrodes, was extended to Ru nanoparticle and Ru/Se electrodes. Using this surface determination it is possible to draw conclusions about the active surface area and the Se composition of the outer shell of Ru/Se nanoparticles.

For the first time we also show, using RRDE measurements, that the oxygen reduction reaction is enhanced by simple Se adsorption also on massive Ru. It could be shown that the activity for the Ru/Se electrode increases with the Se amount on the surface.

Keywords Cu upd · CO oxidation · DEMS · Ruthenium · Selenium · RRDE · Oxygen reduction

N. Bogolowski · T. Nagel · B. Lanova · S. Ernst · H. Baltruschat (✉)
Institut für Physikalische und Theoretische Chemie, Universität Bonn, Römerstrasse 164, 53117, Bonn, Germany
e-mail: baltruschat@uni-bonn.de

K. S. Nagabhushana
Max-Planck-Institut für Kohlenforschung, Kaiser-Wilhelm-Platz-1, 45470, Mülheim an der Ruhr, Germany

Present Address:
K. S. Nagabhushana
Department of Chemistry, Manipal Institute of Technology, Manipal 576104, Karnataka, India

H. Boennemann
Forschungszentrum Karlsruhe, ITC-CPV, D 76021, Karlsruhe, Germany

1 Introduction

$RuSe_x$ catalysts have attracted much attention recently because of their activity for oxygen reduction combined with their complete inactivity for methanol oxidation, which makes them interesting for use as cathode material in the DMFC [1–3]. From a fundamental point of view, it is important to know what makes these catalysts much more active for oxygen reduction than pure Ru. Are special preparation procedures necessary for generating active Ru/Se catalysts or will a simple adsorption of Se onto Ru also lead to an increase of activity? In order to compare the activity of these catalysts the true surface area has to be known.

$RuSe_x$ nanoparticles have been prepared according to various procedures [2–5]. They have been characterized using a variety of methods, including TEM, EXAFS, HRTEM, and XPS [6–9]. However, the surface composition cannot be determined this way. For a catalyst with an unknown surface composition, the classical methods which are based on a defined surface specific property, cannot be

used for the determination of the surface area. The double layer capacity changes strongly with surface composition change. The same is true for pseudo-capacitive charges such as hydrogen and oxygen adsorption, which are often used for the determination of the surface area of Pt and Au. For pure Ru and PtRu alloys, a method based on upd of Cu was described by Kucernak and coworkers [10, 11]. We have shown [12] that this method cannot be simply transferred on $RuSe_x$ catalysts, because the amount of Cu, which can be deposited in the upd-range, decreases with the surface concentration of Se. However, we also outlined a procedure which might serve to determine both the relative surface concentration and the real surface area. This method is based on the determination of Ru surface sites by adsorption of CO and its determination from the amount of CO_2 detected mass-spectrometrically. In addition, the Cu upd charge is determined. From this value the theoretical charge for Cu upd on free Ru sites (as determined from the adsorption of CO) is subtracted: the residual Cu-deposition charge corresponds to Cu upd on Ru completely covered by Se which is one fourth of the value for Cu upd on the bare Ru. It is the purpose of the present work to elucidate whether this method can be applied to nanoparticle catalysts.

Recently, Wieckowski and coworkers [13] examined the catalytic activity of $RuSe_x$ and Ru nanoparticles modified by Se towards O_2 reduction as well as a smooth polycrystalline Ru electrode modified by Se. They found that the Se-modified Ru particles had a similar activity as the $RuSe_x$ particles. However, the smooth Se-modified electrode did not show a higher activity than clean Ru. Therefore in addition we present RRDE measurements which demonstrate that simple adsorption of Se onto rough Ru electrodes leads to a considerable enhancement in catalytic activity. The activity of $RuSe_x$ particles was examined previous by RRDE [1, 5].

2 Experimental

2.1 RRDE measurements

RRDE measurements on oxygen reduction (ORR) at the Ru/Se-electrodes were conducted in a homemade three-electrode electrochemical cell with a Pt counter electrode and a reversible hydrogen electrode as reference electrode to which all potentials are referred. The working electrode was a Pine MTI34 Series RRDE with interchangeable disc (6 mm diameter, geometrical area 0.283 cm^2) and a Pt-ring (inner diameter 7.55 mm, outer diameter 8.55 mm) on an AFMSRX Rotator. A bipotentiostat model 636 from Pine served as potentiostat for the disc- and ring-electrode. A collection efficiency of $N = 0.22$ was determined experimentally using the reduction of copper(II)-ions in potassium chloride solution, in reasonable agreement with the theoretical value of 0.24. As disc substrate we used a smooth polycrystalline gold disc. Prior to each preparation of a Ru electrode, the ring-disc assembly was dipped for at least 30 min in 5 M KOH, rinsed carefully with Millipore water and both—disc and ring—cycled between 50 and 1550 mV in 0.5 M H_2SO_4 with a scan-rate of 50 mV s^{-1}, until we obtained clean cyclic voltammograms (CVs) for the disc and the ring.

Multilayers of Ru on the Au disc were deposited at 50 mV (deposition time 20 min) from a solution of 5×10^{-3} M $RuCl_3$ in 0.5 M H_2SO_4 (without rotation), resulting in silver-grey electrode with a roughness factor $R_f \approx 8$–14. After deposition of Ru, the true surface area of the electrode was determined by performing a Cu upd experiment in 1×10^{-3} M $CuSO_4$ in 0.5 M H_2SO_4 according to [12]. In short, the electrode was cycled in the copper-containing solution with a scan rate of 5 or 10 mV s^{-1} between 50 and 800 mV. The potential was then stopped for 1 min at the lower limit (to reduce the residual oxide/hydroxide on the Ru) and afterwards at 300 mV in the anodic-scan for 1–10 min. From the charge Q_{Ru}^{Cu} for the Cu upd dissolution (assuming a charge of 520 $\mu C\ cm^{-2}$ for the full Cu-monolayer, see below), the true electrode area was calculated.

Se was deposited on the Ru-modified Au substrate by potential cycling between 50 and 800 mV with a scan-rate of 50 mV s^{-1} for several potential cycles in H_2SeO_3-containing solution with concentrations between 1×10^{-5} and 1×10^{-6} M in 0.5 M H_2SO_4. A further Cu upd experiment was performed on this Se modified surface: comparing the charge from this experiment with that obtained from Cu upd on the Se-free Ru electrode allows calculation of the Se coverage, because the Cu upd charge on the fully Se covered surface is only one fourth of that on the bare Ru (Se coverages below 1 monolayer do not modify the surface area of the Ru substrate). During Ru and Se deposition and characterization of the electrodes in a Cu upd experiment, the potential of the Pt ring was held at 1200 mV to prevent deposition of Ru, Se or Cu.

The prepared and characterized Ru or Ru/Se electrodes were used for the investigation of oxygen reduction by recording current–potential-curves during potential cycling between 50 and 800 mV in oxygen-saturated 0.5 M H_2SO_4 under 1 atm of O_2 with a scan rate of 10 mV s^{-1}. The H_2O_2 production was monitored at the ring held at a constant potential of 1200 mV.

2.2 DEMS measurements

Measurements were carried out with DEMS using a thin layer cell. The dual thin layer flow through cell used in the present study was described in detail elsewhere [14–16].

This cell was used for DEMS in combination with a quadrupole mass spectrometer (Pfeiffer Vacuum QMG 422). The electrolyte volume and the nominal geometric surface area (0.28 cm^2) of the working electrode are defined by a thin (50–100 μm) PTFE ring on the disc shaped working electrode. The reference electrode was a reversible hydrogen electrode (RHE). Two Pt wires were used as counter electrodes. The experiments were performed at room temperature, with a potential sweep rate of 10 mV s^{-1}. The upper limit of the potential scans was set to 900 mV for all Ru containing catalysts in order to avoid dissolution of Ru.

Carbon supported Ru nanoparticle (20 wt% Ru) and Ru/Se nanoparticle (22–31 wt%) were prepared by the Bönnemann group [8, 17]. For the electrode preparation, a definite volume (in the range of 20–30 μl) of an ultrasonically dispersed catalyst in ethylene glycol (Ru) or water (Ru/Se) was pipetted onto the glassy carbon substrate, creating a catalyst film with ruthenium or ruthenium/selenium loading of 10 μg_{metal} cm^{-2}. After evaporating the solvent (at 80–120 °C for ethylene glycol and at 30 °C for water), the deposited catalysts were covered with 84 μl of Nafion solution in water. The resulting Nafion film with a thickness of about 1 μm (for catalyst from ethylene glycol suspensions) or 0.2 μm (for catalysts from water), was of sufficient strength to permanently attach the catalyst particles to the glassy carbon electrode [18].

Multilayers of Ru on Pt were deposited at 50 mV (same Ru solution as above, but at a constant electrolyte flow of 5 μl s^{-1}; deposition time 10 min) resulting in approximately 20% rougher surface than the bare Pt surface. The roughness factor was determined by relating the CO oxidation charge to the geometric area of the electrode surface. The reason for the smaller roughness factor as compared to that obtained at Au disc for RRDE measurements probably is the increased convection. CO was adsorbed at a constant electrode potential of 70 mV by replacing the 0.5 M H_2SO_4 solution with a 0.5 M H_2SO_4 solution saturated with CO (ca. 10^{-3} M). After the formation of a CO monolayer, the solution was exchanged by pure 0.5 M H_2SO_4 solution under potential control (E = 70 mV), in order to have a solution free of CO. Then the adsorbed CO was oxidized to CO_2 during the positive potential sweep. A CO oxidation experiment on polycrystalline Pt is done as well, it serves for the determination of the calibration constant K^* of the experimental setup [16, 19]. K^* is the ratio between the integrated ionic current (Q_i) of the mass spectrometer and the Faradaic current ($Q^{f,CO}$) when the current efficiency is 100%, taking into account the number of electrons (z = 2 for the oxidation of CO) and that 20% of the charge obtained by integration of the background corrected current is still due to double layer charging on Pt. The currents were integrated between 350 and 900 mV.

$$K^* = \frac{zQ_i}{Q^{f,CO}} \text{ and } Q^{f,CO}(\text{calculated}) = \frac{zQ_i}{K^*} \quad (1)$$

Se was deposited by adsorbing a full monolayer at open circuit or by a gradual deposition under potential control. In procedure A, the gradual deposition of Se in the thin layer flow through cell used for DEMS involved potential-cycling between 50 and 300 mV for several cycles in 5×10^{-7} M H_2SeO_3 in 0.5 M H_2SO_4. In procedure B a full monolayer was adsorbed from 10^{-4} M H_2SeO_3 and 0.5 M H_2SO_4 at open circuit potential.

All solutions were prepared using ultrapure water (Millipore; 18.2 MΩ cm, <3 ppb TOC) and ultrapure analytical grade or suprapure chemicals from Merck and Fluka, and deaerated by high purity (99.999%) Ar. O_2 (99.999%) from Praxair was used for preparing oxygen saturated solutions. CO of 99.997% purity from Praxair was used for preparing CO saturated solutions.

3 Results

3.1 Surface determination for Se modified Ru nanoparticle electrodes

Oxidation of CO adsorbed on Ru nanoparticles or Ru nanoparticles modified by Se according to procedure A is shown in Fig. 1. As shown before in [12] for Pt and Ru multilayers on Pt the amount of adsorbed CO decreases with increasing Se coverage. At full coverage of Se no more CO adsorption is observed. The true surface area of Se free catalysts was calculated from the ionic charge for m/z = 44 according to:

$$A_{t,CO} = \frac{2Q_i}{K^* zF\Gamma_M} = \frac{2Q_i}{K^* 280\ \mu C\ cm^{-2}} \quad (2)$$

where F: Faraday constant; Γ_M: 1.45 nmol cm^{-2}.

We assume the same maximum packing density of CO on Ru as on Pt, i.e., 1.45 nmol cm^{-2}, corresponding to 280 μC cm^{-2}. This is 0.66 ML CO adsorbing on Pt (CO molecules per Pt sites), an average value often observed on different smooth and stepped surfaces of platinum [20–22].

For comparison, the area was also calculated from the Faradaic oxidation charge:

$$A_{t,CO}^{faradaic} = \frac{Q^{f,CO}}{280\ \mu C\ cm^{-2}} \quad (3)$$

For the Se modified nanoparticle, the relative Se coverage was determined from the coadsorption experiments with CO. Since CO does not adsorb on Pt [23] or Ru fully covered by Se, the CO oxidation charge on surfaces partially covered by Se corresponds to the free Pt or Ru sites. Since the real surface area does not change by

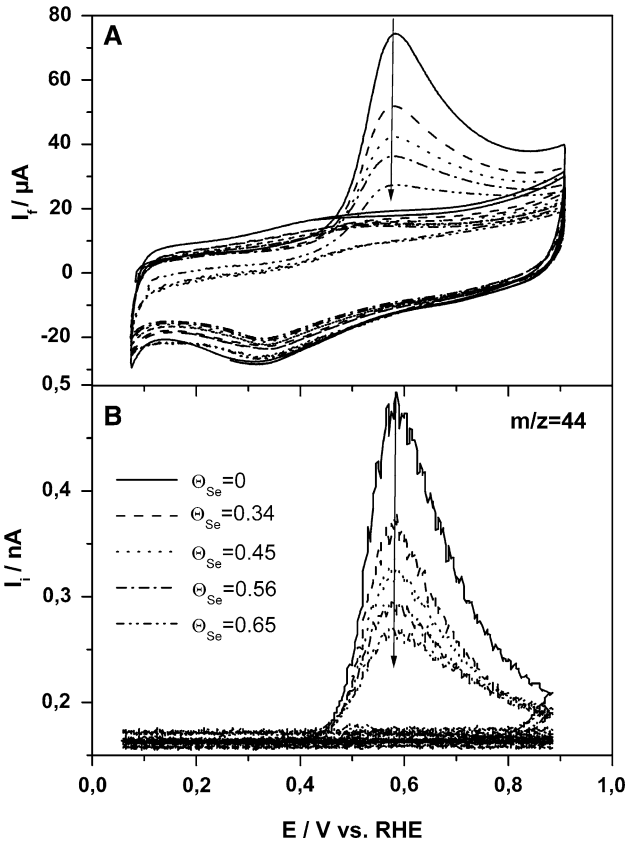

Fig. 1 Simultaneously recorded CV (**A**) and MSCV (**B**) for CO oxidation on Ru nanoparticle (EUP AA225-02, FZ Karlsruhe) with different coverage of Se (Se deposition by procedure A), DEMS-cell, 10 mV s^{-1}, 0.5 M H_2SO_4

modification with Se, the area is given by that determined before from the Se free Ru catalysts. Therefore, with $\Theta_{Se} + \Theta_{CO} = 1$,

$$\Theta_{Se} = 1 - \frac{Q^{CO}_{RuSe}}{Q^{CO}_{Ru}} = \frac{Q^{CO}_{Ru} - Q^{CO}_{RuSe}}{Q^{CO}_{Ru}} \quad (4)$$

Here, Q^{CO} is the true Faradaic CO oxidation charge without double layer contributions as calculated from the mass spectrometric ionic charge.

Experiments for upd of Cu on these surfaces are shown in Fig. 2. Similarly to the CO oxidation charge the Cu upd desorption charge decreases with increasing Se coverage. The Ru nanoparticles thus behave identical to electrodeposited Ru [12].

The charge for the Cu upd desorption peak was determined by integration from 300 to 900 mV. From Cu upd the surface area of Pt electrode is calculated as suggested by Kucernak [11]; the background was not subtracted because the Cu upd layer will be covered by anions at 300 mV as well as Pt at 900 mV; on the contrary, Pt at 300 mV is hardly covered by anions because the value is close to the pzc.

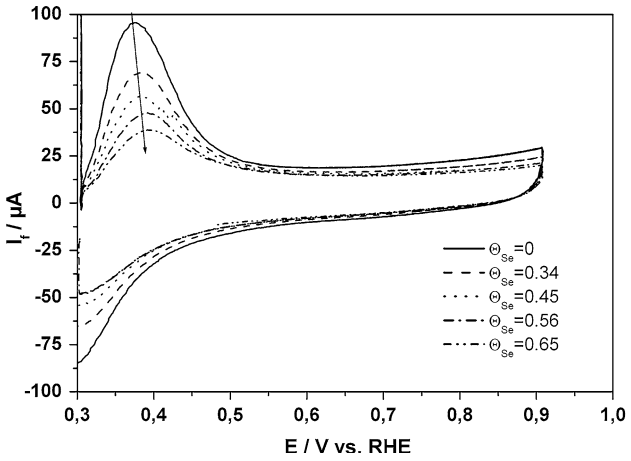

Fig. 2 CV for Cu upd on Ru nanoparticle (EUP AA225-02, FZ Karlsruhe) with different coverage of Se (Se deposition by procedure A), DEMS-cell, 10 mV s^{-1}, 0.5 M H_2SO_4, 10^{-3} M $CuSO_4$, E_{ad} = 300 mV, t = 180 s

$$A_{t,Cu} = \frac{Q^{Cu\ upd}}{420\ \mu C\ cm^{-2}} \quad (5)$$

This value was experimentally verified by comparison of surface areas as obtained from oxidation of adsorbed CO.

For pure Ru the use of the Cu upd charge for the determination of the surface area is less straightforward because of the much higher pseudo-capacitive contributions. The average experimental value (after background subtraction) obtained from 6 independent measurements gave a value of 520 $\mu C\ cm^{-2} \pm 15\%$. Here, the surface area was determined from the amount of adsorbed CO as measured by DEMS as described above. This value can be understood by taking into account that the packing density of Cu on Ru is increased by 5% as compared to Pt due to the smaller atomic distance. (On the contrary, the packing density of CO is determined by its size and not the density of the substrate atoms.) As in the case of CO oxidation, the oxidation charge after background subtraction furthermore contains a large capacitive contribution; in [12] we had shown that at 350 mV the anionic charge on Ru corresponds to about 1 electron per Ru atom, certainly much more than on the Cu monolayer. For the calculations we therefore use:

$$A_{t,Cu} = \frac{Q^{Cu\ upd}}{520\ \mu C\ cm^{-2}} \quad (6)$$

Table 1 summarizes data obtained from four different electrode preparations with Ru nanoparticles in comparison to Ru electrodes obtained from Ru multilayer electrodeposition on Pt. In all cases the oxidation charge calculated from the amount of formed CO_2, i.e., from the integrated mass spectrometric ion current is only 45% of the total Faradaic charge. This implies that more than the half of the Faradaic charge is due to capacitive effects.

Table 1 Summary of the charges and the calculated electrodes surface areas by CO oxidation and Cu upd

Substrate	Charge (mC)			$Q^{f,CO}$ (calc.)/ $Q^{f,CO}$	Surface area (cm^2)			$A_{t,CO}/A_{t,Cu}$	Q^{CO}/Q^{Cu}
	Q^{Cu}	$Q^{f,CO}$ (calc.)	$Q^{f,CO}$		$A_{t,Cu}$ from Q^{Cu}	$A_{t,CO}$ from $Q^{f,CO}$ (calc.)	$A_{t,CO}$ from $Q^{f,CO}$		
Ru multilayers	0.226	0.098	0.219	0.45	0.44	0.35	0.78	0.81	0.44
Ru multilayers	0.152	0.086	0.206	0.42	0.29	0.31	0.74	1.05	0.57
Ru multilayers	0.193	0.112	0.223	0.50	0.37	0.40	0.80	1.08	0.58
Ru nanoparticle[a]	1.442	0.703	1.502	0.45	2.77	2.51	5.36	0.91	0.49
Ru nanoparticle[b]	0.803	0.498	1.231	0.40	1.54	1.78	4.40	1.15	0.62
Ru nanoparticle[a]	1.870	0.960	2.321	0.41	3.60	3.43	8.29	0.95	0.51
Ru nanoparticle[b]	0.844	0.510	1.090	0.47	1.62	1.21	3.90	1.12	0.60
Pt nanoparticle[c]	1.349	0.782	1.023	0.75	3.21	2.82	3.69	0.88	0.58
Pt nanoparticle[c]	1.101	0.621	0.821	0.76	2.62	2.24	2.96	0.85	0.56
Pt nanoparticle[c]/Ru[d]	1.018	0.574	0.779	0.74	2.42	2.07	2.81	0.85	0.56
Pt nanoparticle[c]/Ru[e]	0.930	0.544	0.738	0.74	2.21	1.96	2.66	0.88	0.58

$Q^{f,CO}$(calc): CO oxidation charge calculated from the mass spectrometric ionic charge Q_i for the amount of CO_2

$Q^{f,CO}$: Faradaic CO oxidation charge

$Q^{Cu\ upd}$: Cu upd desorption charge

$A_{t,CO}/A_{t,Cu}$: Ratio of surface areas determined by CO oxidation and Cu upd

[a] Ru, 20 wt%, EUP AA205-02, FZ Karlsruhe

[b] Ru, 20 wt%, EUP AA225-02, FZ Karlsruhe

[c] Pt, 40 wt% ETEK #C0510517

[d] $\Theta_{Ru} = 0.25$

[e] $\Theta_{Ru} = 0.45$

Surface areas calculated from the Cu upd charge agree with a small deviations with those obtained for the CO oxidation charge (calculated from mass-spectrometry). We checked that the amount of Cu upd is not influenced by the adsorbed oxides or hydroxides on the ruthenium surface during the adsorption of the bulk and the copper monolayer: In control experiments the Cu^{2+} solution was introduced at 50 mV instead of 300 mV; the obtained charge values for Cu upd deviate from each by less than 10% only.

Values of the Cu upd charge on Ru nanoparticle electrodes modified with different amounts of Se are plotted as a function of the Se coverage in Fig. 3A (Θ_{Se} was calculated from the suppression of CO adsorption). For comparison, values for electrodeposited Ru modified with Se are also included. For both types of electrodes the same relationship is obtained. The extrapolation to $\Theta_{Se} = 1$ gives a charge of roughly 130 $\mu C\ cm^{-2}$ for Cu upd on selenium, this is a fourth of the Cu upd charge on the bare ruthenium or platinum surfaces.

The reason for the decrease to one fourth of the charge on the Se free surface is still unclear. We showed that the Cu deposition charge for Se modified Pt or for Ru monolayers modified with Se does not vary with Se coverage, as long as no copper selenide is formed [12]. (Here, Cu probably is deposited underneath the Se adlayer, similar to Cd upd on the Se modified Au surfaces [24] or Ag upd onto iodine modified Pt(111) surface [25].) The decrease might be due to a surface phase which is only formed when Se is adsorbed onto multilayers of Ru (or bulk Ru). For Se coverage higher than 0.9 the Cu upd charge increases due to the formation of $CuSe_x$.

Figure 3B shows that such a decrease is not observed for Pt or Pt surfaces modified by Ru, including Pt nanoparticles, suggesting that in the case of Ru electrodes deeper Ru layers are involved in the formation of a particular $RuSe_x$ phase.

If the amount of Cu upd was independent of Se coverage the true surface area for a catalyst of unknown surface composition could be calculated simply from the upd charge; the surface coverage of Se could then be calculated from the surface coverage of CO according to

$$\Theta_{Se} = 1 - \Theta_{CO} \tag{7}$$

Here (and also below) it is assumed, that CO and Se do not interact with each other, i.e., that a surface site is either occupied by CO molecule or a Se atom, a condition which is best fulfilled if both species form domains on the surface. This may be justified from the linear dependence of the hydrogen adsorption charge on the Se coverage on Pt surfaces [12, 23].

Nevertheless, the true surface area and the Se surface coverage can be calculated from the Cu upd charge and the amount of coadsorbed CO as follows.

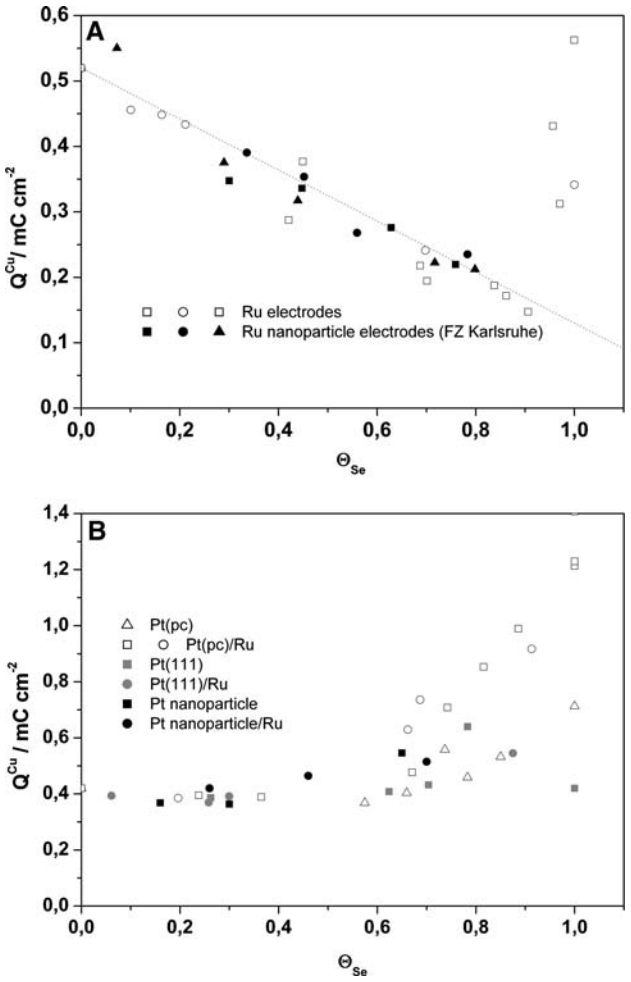

Fig. 3 Charge of Cu upd dissolution versus Θ_{Se} calculated from the suppression of CO adsorption. (**A**) Different preparations for Ru nanoparticle electrodes (filled symbols/■ ● ▲) and multilayers of Ru on Pt electrode (open symbols/□ ○ △) and (**B**) submonolayers of Ru on △ Pt(pc), □ ○ Pt(pc)/Ru, ■ Pt(111), ● Pt(111)/Ru, ■ Pt nanoparticle electrodes and ● Pt nanoparticle electrodes/Ru

We regard the surface area as a composition of a part with Se atoms on top and another part with pure Ru sites. Since CO adsorbs only on the Ru sites, this part of the surface area can described by the CO oxidation charge. From the Cu upd charge for a Ru electrode covered by a monolayer of Se is the Se covered part of the total area:

$$A_{Se} = \frac{Q_{Se}^{Cu}}{130\ \mu C\ cm^{-2}} \tag{8}$$

The part of Se sites can be determined via the Cu upd charge. Taking into account Eqs. 3 and 8, we get

$$A_{total} = A_{Ru} + A_{Se} = \frac{Q_{Ru}^{CO}}{280\ \mu C\ cm^{-2}} + \frac{Q_{Se}^{Cu}}{130\ \mu C\ cm^{-2}} \tag{9}$$

The Cu upd desorption charge on the Se part of the surface cannot be determined directly since Cu upd takes place on Ru surface atoms as well. Using Eq. 6 we get

$$\begin{aligned} Q_{total}^{Cu} &= Q_{Se}^{Cu} + Q_{Ru}^{Cu} \text{ or } Q_{Se}^{Cu} = Q_{total}^{Cu} - Q_{Ru}^{Cu} \\ &= Q_{total}^{Cu} - (A_{Ru} 520\ \mu C\ cm^{-2}) \end{aligned} \tag{10}$$

A_{Ru} is determined using again Eq. 3.

$$Q_{Se}^{Cu} = Q_{total}^{Cu} - \frac{Q_{Ru}^{CO}}{280\ \mu C\ cm^{-2}}\ 520\ \mu C\ cm^{-2} \tag{11}$$

Thus, the measurement of the CO oxidation charge and of the total charge for Cu upd yield the areas of the Se covered Ru and the bare Ru:

$$A_{Ru} = \frac{Q_{Ru}^{CO}}{280\ \mu C\ cm^{-2}} \tag{12}$$

and

$$A_{Se} = \frac{Q_{total}^{Cu} - \frac{Q_{Ru}^{CO}}{280\ \mu C\ cm^{-2}}\ 520\ \mu C\ cm^{-2}}{130\ \mu C\ cm^{-2}} = \frac{Q_{total}^{Cu} - \frac{13}{7} Q_{Ru}^{CO}}{130\ \mu C\ cm^{-2}} \tag{13}$$

From this the total area (A_{total}) and the relative Se coverage is calculated:

$$\Theta_{Se} = \frac{A_{Se}}{A_{total}} \tag{14}$$

Alternatively, the derivation is as follows:

The experimentally determinable charge values are given by:

$$\begin{aligned} Q^{CO} &= A_{total}\ \Theta_{CO}\ 280\ \mu C\ cm^{-2} \\ &= A_{total}(1 - \Theta_{Se})\ 280\ \mu C\ cm^{-2} \end{aligned} \tag{15A}$$

$$\begin{aligned} Q^{Cu} &= A_{total}\ (1 - \Theta_{Se})\ 520\ \mu C\ cm^{-2} \\ &+ A_{total}\ \Theta_{Se}\ 130\ \mu C\ cm^{-2} \end{aligned} \tag{15B}$$

these are two equations which can be solved for the two unknowns Θ_{Se} and the total area A_{total}. The ratio of these two charges does not depend on the total area or the amount of catalyst:

$$\begin{aligned} \frac{Q^{CO}}{Q^{Cu}} &= \frac{A_{total}\,(1-\Theta_{Se})\,280\,\mu C\,cm^{-2}}{A_{total}\,(1-\Theta_{Se})\,520\,\mu C\,cm^{-2} + A_{total}\,\Theta_{Se}\,130\,\mu C\,cm^{-2}} \\ &= \frac{28(1-\Theta_{Se})}{52-39\Theta_{Se}} \end{aligned} \tag{16}$$

This function may be used as a calibration curve from which the surface concentration can be determined. Experimental values (from the data shown in Fig. 3A) for

our Se modified Ru catalysts (for which the surface area had been determined before Se modification and the Se coverage is known) are plotted in Fig. 4A. The data agree quite well with the mathematical function of Eq. 16. (For comparison, values for the charge ratio are also shown for Pt and Ru modified Pt electrodes in Fig. 4B.)

We then used this approach to estimate the surface concentration of different $RuSe_x$ nanoparticle electrodes. The data are summarized in Table 2.

Table 2 Comparison of the electrode surface areas and surface composition of $RuSe_x$ catalysts with different Ru:Se atomic ratios

Ru:Se	x_{Se}	Q^{CO}/Q^{Cu}	Θ_{Se}
1:0.15	0.13	0.474 ± 0.038	0.34 ± 0.17
1:0.3	0.23	0.445 ± 0.025	0.45 ± 0.11
1:0.59	0.37	0.398 ± 0.010	0.53 ± 0.24
1:1	0.50	0.02	0.99

3.2 ORR measurements

In order to test whether simple adsorption of Se from selenic acid solution on Ru results in an increased catalytic activity, RRDE measurements were carried out. After deposition of Ru on Au cyclic voltammetric curves (CVs) were recorded in 0.5 M H_2SO_4 with a scan rate of 50 mV s^{-1}, until two consecutive cycles were indistinguishable. Se was deposited during 3–4 potential cycles from selenic acid (of varying concentrations). Examples for the final cycles before characterizing the electrode in a Cu upd experiment and transferring the electrode into oxygen saturated sulfuric acid are shown in Fig. 5. For comparison the currents were normalized to the true surface area of the bare Ru electrode. With increasing Se coverage, the pseudo-capacitive currents due to hydrogen and anion adsorption/desorption are suppressed. These pseudo-capacitive processes also take place during ORR. Therefore, the corresponding currents are always subtracted from the experimental currents for the oxygen reduction.

Examples for the ORR in oxygen-saturated 0.5 M H_2SO_4 on the Ru- and Ru/Se electrodes are shown in Fig. 6. On the bare Ru surface the diffusion limited currents are not reached even at low potentials (high overpotentials). However, after deposition of Se on Ru the catalytic activity is increased in the whole potential range between 800 and 100 mV.

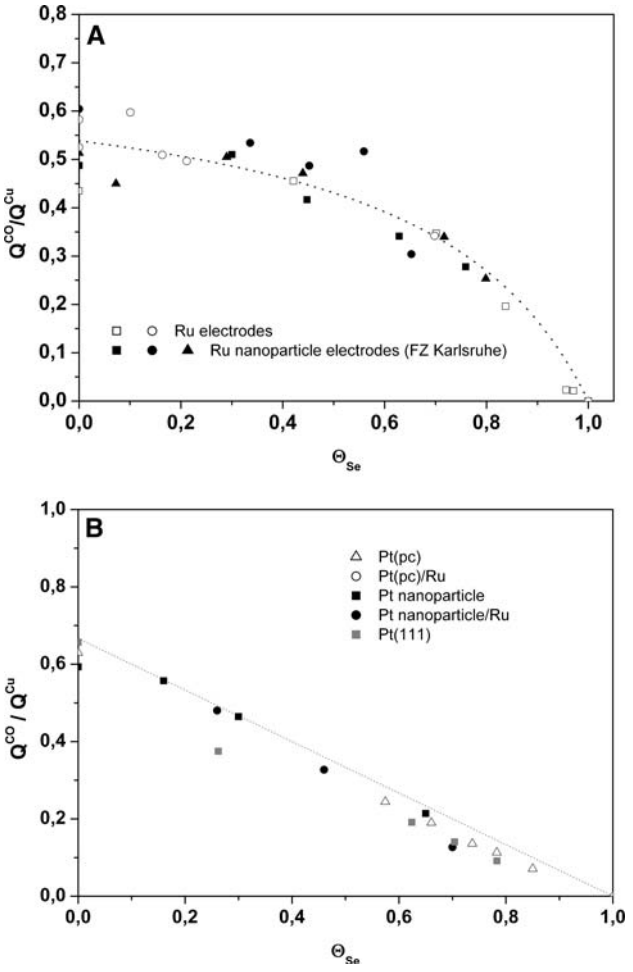

Fig. 4 Ratio of the Cu upd charge and CO oxidation charge versus Θ_{Se} calculated from the suppression of CO adsorption. For different substrates with gradual deposited Se. (**A**) Different preparations for Ru nanoparticle electrodes (■ ● ▲ FZ-Karlsruhe) and multilayers of Ru (□ ○) and (**B**) ■ Pt-nanoparticle electrode, ○ Pt(pc)/Ru, △ Pt(pc) and ■ Pt(111)

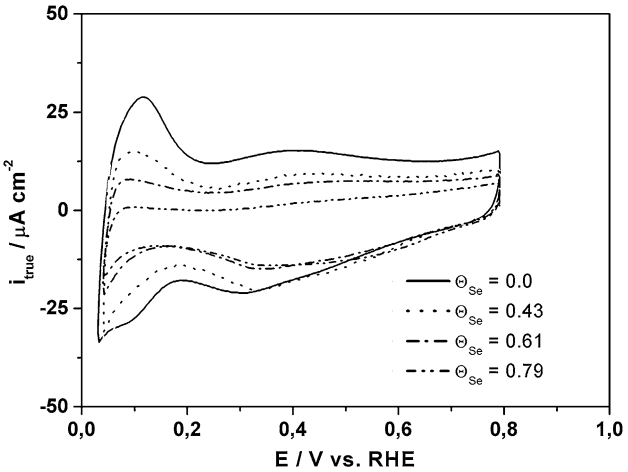

Fig. 5 CVs of the Au disc covered with multilayers of Ru and different coverage of Se in argon-saturated 0.5 M H_2SO_4 (Θ_{Se} = 0.0) and 1×10^{-5} M H_2SeO_3 in 0.5 M H_2SO_4 (last cycle before emersion, Θ_{Se} = 0.43, 0.61 and 0.79). dE/dt = 50 mV s^{-1}. Currents normalized to true surface area. R_f = 8.1

The ratio of the hydrogen peroxide production related to the overall reaction is calculated according to [26],

$$X_{H_2O_2} = \frac{2(I_{ring}/N)}{I_{disc} + (I_{ring}/N)} \quad (17)$$

where absolute values of the currents are used and $N = 0.22$. They are shown in Fig. 7. With decreasing potentials (increasing overpotential) the hydrogen peroxide production decreases drastically from around 80% ore more to less than 10%. At potentials above 650 mV (low overpotential) increasing Se coverage on Ru decreases the hydrogen peroxide production, while at lower potentials (high overpotential) the low hydrogen peroxide production is somewhat increased with higher Se coverage.

Due to the very small currents above 700 mV, small errors, e.g., in the baseline correction may lead to considerable changes (up to a factor of 2) in the amount of H_2O_2 production. The tendency in the effect of Se coverage (bare Ru highest H_2O_2 amount, Ru/Se lower amounts) is not affected. In the potential regime below 700 mV the values for H_2O_2 production are hardly affected by a different background subtraction.

The kinetic currents were obtained using the Koutecky-Levich analysis [27] of the disc currents (cf. inset in Fig. 8):

$$\frac{1}{I_{disc}} = \frac{1}{I_{kin}} + \frac{1}{B\omega^{1/2}} \quad (18)$$

where I_{kin} is kinetic current density and $B = 0.62nFCD^{2/3}\nu^{-1/6}$ is a constant slope, n = number of electrons transferred per oxygen molecule, F = Faraday constant, c = oxygen-concentration in 0.5 M H_2SO_4, D = diffusion coefficient for oxygen in 0.5 M H_2SO_4, ν = kinematic viscosity of 0.5 M H_2SO_4 and ω = angular rotation frequency, for a Ru/Se electrode with $\Theta_{Se} = 0.43$ are shown as inset in Fig. 8. For B we found experimentally $B = 420.3$ μA cm^{-2} rad$^{1/2}$ s$^{-1/2}$ at low potentials (high overpotentials). From the intercepts with the extrapolation to infinite rotation of the Koutecky-Levich-plots of $1/i$ versus $w^{-1/2}$, plotted as a function of the electrode potential, we obtain the kinetic currents. These mass transfer corrected kinetic currents were normalized to the true surface area, as described in the experimental section and in [12]. Resulting Tafel-plots of the different Ru and Ru/Se electrodes are shown in Fig. 8.

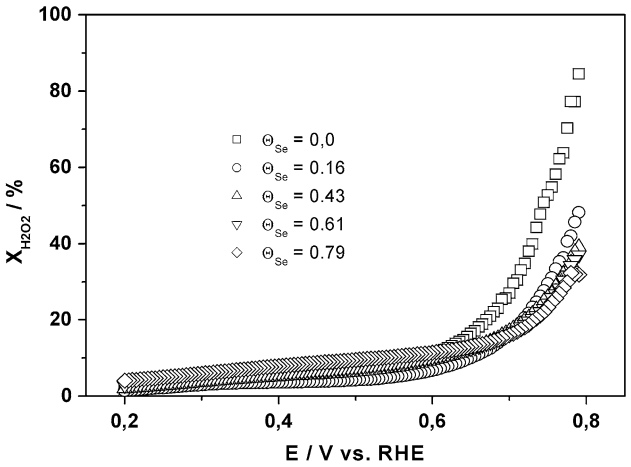

Fig. 7 H_2O_2 production as function of the electrode potential obtained from disc and ring currents at 3000 RPM for Ru and different Ru/Se electrodes. dE/dt = 10 mV s^{-1}

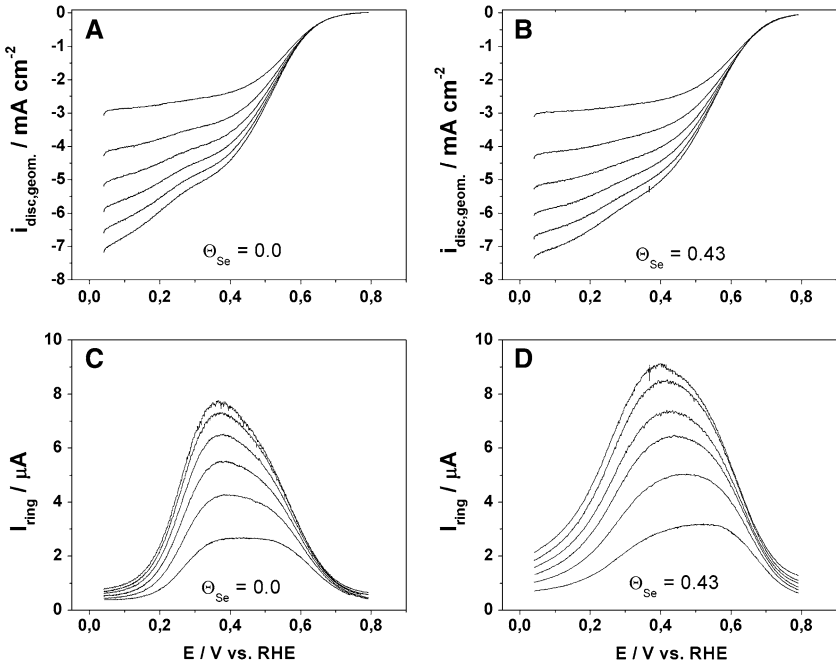

Fig. 6 Characteristic current–potential-curves for the disc (**A** and **B**) and ring currents (**C** and **D**) for ORR on Ru and Ru/Se electrodes ($\Theta_{Se} = 0.43$) in oxygen-saturated 0.5 M H_2SO_4 at 500, 1000, 1500, 2000, 2500 and 3000 RPM. dE/dt = 10 mV s^{-1}. Disc currents normalized to the geometric area of the electrode (0.283 cm^2). Ring electrode potential: 1.2 V

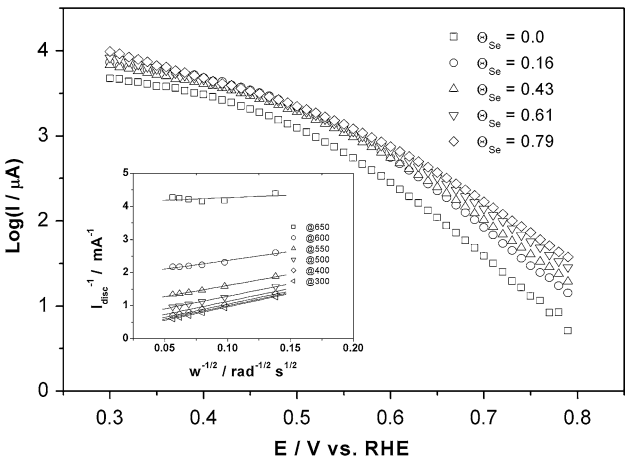

Fig. 8 Tafel-plot of the kinetic currents obtained from the intercept from Koutecky-Levich-plots for the Ru and Ru/Se electrodes with different Se coverage. Inset: Koutecky-Levich-plots for the Ru/Se electrode (Θ_{Se} = 0.43) at 300, 400, 500, 550, 600 and 650 mV

In the potential range above 600 mV (lower overpotentials) the Tafel-slope varies from −110 mV dec^{-1} for Θ_{Se} = 0 to −138 mV dec^{-1} for Θ_{Se} = 0.79. The slopes are comparable to those of −120 mV dec^{-1}, respectively, found by Damjanovic for ORR on massive polycrystalline platinum [28] or by Markovic and Ross [29] found for Pt(111) and −124 mV dec^{-1} found for electrochemical deposited ruthenium-films on gold electrodes by Metikos-Hukovic [30].

As shown in Fig. 9 the normalized current densities depend nearly linear on the Se coverage.

4 Discussion

As can be seen from Table 2, the $RuSe_x$ nanoparticles display a much higher surface concentration of Se than given by the bulk composition. This might be understood from a segregation of Se to the surface. It was estimated [8] that even the $RuSe_{0.15}$ catalyst would then have a Se-surface concentration of 0.5, this is in good agreement with our results. With such a reasoning, one would expect high surface concentrations for catalysts with low Se content. From HRTEM, it was concluded that small $RuSe_2$ clusters exist on the surface of the particles. Correspondingly, the Se-concentration elsewhere in the particle will be lower. Therefore also the Se surface concentration will be lower than expected from a simple model involving Se segregation to a surface monolayer. Certainly, our estimate for the total surface area still has to be considered with some care. At this point it is not clear whether Cu also can be deposited on the surface of such a $RuSe_2$-face.

The increase in the catalytic activity after Ru modification is interesting, because catalysts with the same known real

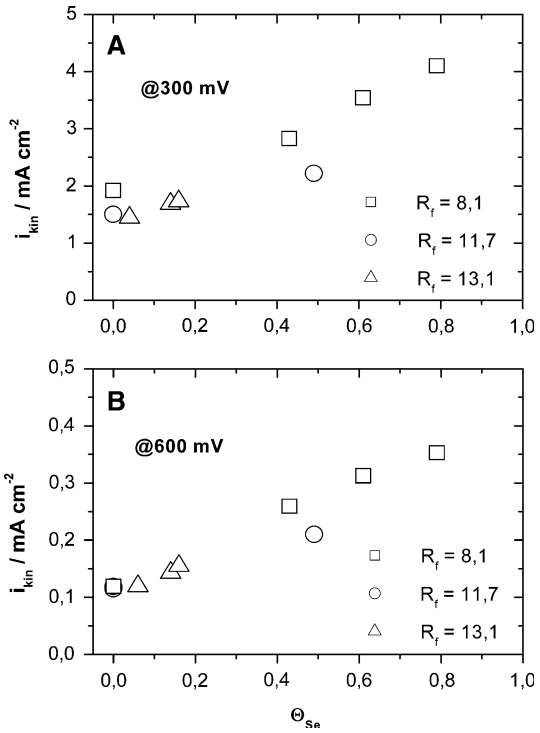

Fig. 9 Kinetic current densities obtained from the Tafel-plots (cf. Fig. 8), normalized to the true surface area determined for the bare Ru electrode by Cu upd, as a function of the Se-coverage Θ_{Se} for different electrode potentials: (**A**) 300 mV, (**B**) 600 mV

surface area are compared and the effect therefore cannot be ascribed to an increased surface area. For the $RuSe_x$ catalysts, for which an increased catalytic activity was described in the literature, the true surface area and surface composition was unknown and could not be compared to pure Ru. An increase in the catalytic activity (for Se deposited on Ru black) was also found by Wieckowski and coworkers [13]. They investigated the influence of Se deposited on Ru black on the ORR by stripping of the Se in potential-cycles between 300 and 1200 mV. They did not observe a catalytic effect when a massive Ru electrode was modified by Se. The difference may be due to a different modification procedure (modification by elemental Se in an organic solution whereas we adsorbed Se from aqueous selenide solution) or be due to the fact that our Ru deposit had a much larger roughness factor ($R_f \approx 8$–14) and thus a surface structure which resembles that of Ru black.

The strong dependence of the H_2O_2 formation on potential—a similar dependence was reported in [1]—very much differs from the case of Pt, where H_2O_2 formation increases when hydrogen is adsorbed and the O–O splitting reaction becomes inhibited. This behavior may be due to two different reasons:

(1) Oxygen adsorption inhibits the O–O splitting, the lower the potential, the less oxygen (or hydroxide)

species is adsorbed. The fact that the H_2O_2 formation is suppressed somewhat with increasing Se coverage (which suppresses OH adsorption) supports this interpretation.

(2) Although the Tafel slope of 120 mV suggests that the first electron transfer is the rate-determining step as in the case of Pt, the O–O splitting on the surface is slower than the desorption of H_2O_2. Since the rate constant for the H_2O_2 desorption step should be independent of potential, at decreasing potentials the reduction of H_2O_2 to water becomes appreciable. Two reaction steps therefore are slowed down in comparison to Pt: the rate determining first electron transfer *and* the O–O splitting.

Acknowledgements This work was financed by the BMBF within the framework of the O2 RedNet project. We thank all members of the O2rednet, for stimulating discussions, particularly E. Savinova.

References

1. Bron M, Bogdanoff P, Fiechter S, Hilgendorff M, Radnik J, Dorbandt I, Schulenburg H, Tributsch H (2001) J Electroanal Chem 517(1–2):85
2. Tributsch H, Bron M, Hilgendorff M, Schulenburg H, Dorbandt I, Eyert V, Bogdanoff P, Fiechter S (2001) J Appl Electrochem 31(7):739
3. Neergat M, Leveratto D, Stimming U (2002) Fuel Cells 2(1):25
4. Hilgendorff M, Diesner K, Schulenburg H, Bogdanoff P, Bron M, Fiechter S (2002) J New Mat Electrochem Syst 5(2):71
5. Leveratto D, Racz A, Savinova ER, Stimming U (2006) Fuel Cells 6(3–4):203
6. Malakhov IV, Nikitenko SG, Savinova ER, Kochubey DI, Alonso-Vante N (2002) J Phys Chem B 106(7):1670
7. Alonso-Vante N, Malakhov IV, Nikitenko SG, Savinova ER, Kochubey DI (2002) Electrochim Acta 47(22–23):3807
8. Zaikovskii VI, Nagabhushana KS, Kriventsov VV, Loponov KN, Cherepanova SV, Kvon RI, Bonnemann H, Kochubey DI, Savinova ER (2006) J Phys Chem B 110(13):6881
9. Dassenoy F, Vogel W, Alonso-Vante N (2002) J Phys Chem B 106(47):12152
10. Green CL, Kucernak A (2002) J Phys Chem B 106(44):11446
11. Green CL, Kucernak A (2002) J Phys Chem B 106(5):1036
12. Nagel T, Bogolowski N, Baltruschat H (2006) J Appl Electrochem 36(11):1297
13. Cao D, Wieckowski A, Inukai J, Alonso-Vante N (2006) J Electrochem Soc 153(5):A869
14. Wang H, Löffler T, Baltruschat H (2001) J Appl Electrochem 31:759
15. Jusys Z, Massong H, Baltruschat H (1999) J Electrochem Soc 146:1093
16. Baltruschat H (2004) J Am Soc Mass Spectrom 15:1693
17. Bonnemann H, Nagabhushana KS (2004) J New Mat Electrochem Syst 7(2):93
18. Schmidt TJ, Gasteiger HA, Stab GD, Urban PM, Kolb DM, Behm RJ (1998) J Electrochem Soc 145(7):2354
19. Baltruschat H (1999) In: Wieckowski A (ed) Interfacial electrochemistry. Marcel Dekker Inc., New York, Basel
20. Hartung T, Schmiemann U, Kamphausen I, Baltruschat H (1991) Anal Chem 63:44
21. Schmiemann U (1993) PhD Thesis; Universität Witten-Herdecke
22. Climent V, Gómez R, Feliu M (1999) Electrochim Acta 45:629
23. Herrero E, Rodes A, Pérez JM, Feliu JM, Aldaz A (1996) J Electroanal Chem 412:165
24. Lister TE, Colletti LP, Stickney JL (1997) Isr J Chem 37(2–3):287
25. Hubbard AT, Stickney JL, Rosasco SD, Song D, Soriaga MP (1983) Surf Sci 130:326
26. Murthi VS, Urian RC, Mukerjee S (2004) J Phys Chem B 108(30):11011
27. Bard AJ, Faulkner LR (2001) Electrochemical methods: fundamentals and applications, 2nd edn. John Wiley & Sons Inc., New York, Weinheim
28. Sepa DB, Vojnovic V, Damjanovic A (1981) Electrochim Acta 26:781
29. Markovic MN, Ross PN (1999) In: Wieckowski A (ed) Interfacial electrochemistry. Marcel Dekker, Inc., New York
30. Metikos-Hukovic M, Babic R, Jovic F, Grubac Z (2006) Electrochim Acta 51(7):1157